# Microtubule Behavior in the Growth Cones of Living Neurons during Axon Elongation

**Elly M. Tanaka and Marc W. Kirschner**

Department of Biochemistry and Biophysics, University of California, San Francisco, California 94143

*Abstract.* To understand how microtubules are generated in the growth cone, we have imaged fluorescently tagged microtubules in living frog embryonic neurons. The neurons were labeled by injecting rhodamine-labeled tubulin into the fertilized egg and explanting the neurons from the neural tube. Microtubules extend deep into the growth cone periphery and adopt three characteristic distributions: (*a*) dispersed and splayed throughout much of the growth cone; (*b*) looped and apparently contorted by compression; and (*c*) bundled into tight arrays. These distributions interconvert on a time scale of several minutes and these interconversions are correlated with the behavior of the growth cone. We observed microtubule growth and shrinkage in growth cones, but are unable to determine their contribution to net assembly. However, translocation of polymer from the axon appears to be a major mechanism of generating new polymer in the growth cone, while bundling of microtubules in the growth cone appears to be the critical step in generating new axon. Neurons that were about to turn spontaneously generated microtubules in the future direction of growth, suggesting that orientation of microtubules might be an important early step in neuronal pathfinding.

EARLY investigations of cytoplasmic structure using EM revealed organized arrays of microtubules in asymmetric cells. The arrangement of microtubules suggested that they may play a role in establishing or maintaining cell shape (Porter, 1966). In neurons, which are long asymmetric cells, parallel microtubules were found to run down the axon (Peters et al., 1991). Their importance in establishing and maintaining axonal structure was demonstrated when application of colchicine, a specific microtubule-disrupting agent, caused growing neurites to collapse, and inhibited new neurite outgrowth (Daniels, 1972; Yamada et al., 1971). Despite the acknowledged importance of microtubules in the structure of axons, their exact role in the growth of axons, their mechanism of assembly and transport in the axon, and the possible function of microtubules in the pathfinding decisions made at the growth cone are still unresolved.

Since the early morphological studies of Ramon y Cajal and Harrison (Ramon y Cajal, 1890; Harrison, 1910), the growth cone has been ascribed the major role for generating new axonal structure and for determining the orientation of that structure in pathfinding decisions. Even though microtubules are the major structural elements of the developing axon, it is not yet clear whether microtubules play any role in the pathfinding decisions in the growth cone. Some of the present uncertainty stems from an imprecise knowledge of where microtubules are located in the growth cone. Early studies found that they did not extend beyond the growth cone neck and appeared to be prevented from entering the lamella by a dense network of microfilaments (Bunge, 1973; Yamada et al., 1971). Among the cytoskeletal elements, actin was shown to be present in the growth cone, so it was proposed that the actin cytoskeleton and not the microtubules controls the motility and directionality of the growth cone and thus determines the direction and rate of axonal elongation. In this view, microtubules play a subordinate role: to fill in the axon structure generated by the advancing growth cone. The parallels between the motility of migrating cells, some of which can migrate without microtubules, and the motility of the growth cone, reinforce the idea that microtubules may play a minor role in growth cone guidance.

Other studies indicated that microtubules may play a more active role in the generation and orientation of the growing axon. More recent electron microscopic images show microtubules extending beyond the neck, deep into the growth cone lamella (Bridgman and Dailey, 1989; Cheng and Reese, 1985; Tsui et al., 1984). In time lapse recordings, organelles that presumably move along microtubules were seen to invade the peripheral lamellipodia, suggesting that as the axon grows, microtubules may sometimes populate the distal regions of the growth cone (Goldberg and Burmeister, 1986). In addition, although actin is undoubtedly important for growth cone structure, neurites continue to grow in the presence of cytochalasin B, an actin depolymerizing drug, suggesting that microtubule polymerization or extrusion may itself be able to drive axonal growth (Bentley and Toroian-Raymond, 1986; Marsh and Letourneau, 1984).

The heterogeneous morphology of growth cones has made

it difficult from static light or electron microscopic images to reconstruct the process of neurite outgrowth. Advancing growth cones actively remodel their cortex, continually forming and dissolving their filopodia, lamellipodia, and veils. These processes can be followed by phase or DIC microscopy, but they do not give any indication of the location or dynamics of the microtubules in the cell interior. So far, most studies of microtubules have been limited to the direct observation of fixed specimens by EM or immunofluorescence. In one study (Forscher and Smith, 1988), a limited number of microtubules could be seen in living growth cones after treatment with cytochalasin D and though this study showed that the actin network may restrict access of microtubules to the lamella, it did not examine the assembly of microtubules during normal growth.

It would be of particular interest to follow microtubules in living neurons to understand how they are assembled during neurite outgrowth and to define precisely their role in turning decisions. In other cell types, as well as in the studies of microtubule polymerization in vitro, it has been necessary to visualize and measure individual microtubules over time to appreciate their dynamic characteristics. In growth cones, direct observation can distinguish among several of the proposed models that predict different modes of microtubule stabilization and localization (Mitchison and Kirschner, 1988). We have developed a novel system to label and follow individual microtubules over time in the growth cones of rapidly growing neurons in culture. Here, we report our observations of microtubules in the growth cones of these neurons and discuss the implications of such observations on the mechanism of microtubule extension during axon elongation and turning.

## Materials and Methods

### Tubulin Labeling

Bovine brain tubulin was labeled with 5-(+6)-carboxytetramethylrhodamine succinimidyl ester (C-1171, Molecular Probes, Eugene, OR) essentially as described previously (Hyman et al., 1991). This resulted in a labeling of tubulin with 2 mol of rhodamine per mol of tubulin.

### Labeling and Culturing of Xenopus Neurons

*Xenopus* eggs were fertilized and dejellied in vitro as previously described (Newport and Kirschner, 1982). At the two-cell stage, the eggs were placed in 1× MMR (0.1 M NaCl, 2 mM KCl, 1.0 mM $MgSO_4$, 2.0 mM $CaCl_2$, 5.0 mM Hepes, 0.1 mM EDTA [pH 7.8]), 5.5% ficoll. 50 nl of 5 mg/ml rhodamine-tubulin was injected into one of the two blastomeres using an air pressure injector and calibrated needles. With an estimated content of tubulin in the egg of 1 μg (Gard and Kirschner, 1987), the initial ratio of labeled exogenous tubulin to endogenous tubulin was ~1:4. 1–3 h after injection, the normal eggs were transferred to 0.1× MMR, 5.5% ficoll to allow proper gastrulation, while the abnormally developing embryos (~20%, but highly dependent on egg batch) were discarded. Injected embryos that appeared normal at 3 h developed normally through tadpole stages and beyond. Half of the injected eggs were placed at 18°C, and the other half at 13°C to stagger development. The embryos were allowed to develop in the dark until ST 20–24 (Nieuwkoop and Faber, 1956) (~40 h at 18°C and 64 h at 13°C).

At the neurula stage, the neural tube was dissected as described previously (Hinkle et al., 1981). Briefly, the embryos were placed in Steinberg's solution (58 mM NaCl, 0.67 mM KCl, 0.44 mM $Ca(NO_3)_2$, 1.3 mM $MgSO_4$, 4.6 mM Tris, pH 7.8) for dissection, and using fine forceps, the entire dorsal portion of the embryo was removed and then incubated for 40 min at 19°C in 1 mg/ml collagenase (type 1A, Sigma C-9891; Sigma Chemical Co., St Louis, MO) dissolved in Steinberg's solution. The dorsal portions were then placed back into collagenase-free Steinberg's solution, and the neural tube was teased out using fine forceps. The neural tube was divided along its length into several pieces, and temporarily stored in a small tube containing Steinberg's solution. The neurons were cultured as explants in Steinberg's plating media (20% Leibovitz L-15, 58 mM NaCl, 0.67 mM KCl, 0.44 mM $Ca(NO_3)_2$, 1.3 mM $MgSO_4$, 4.6 mM Tris, pH 7.8, 10 mM $MgCl_2$, 0.1% Gentamycin) with no FCS, on 25-mm round glass coverslips (no. 1). The coverslips had first been acid washed with 1 N HCl for 6 h at 65°C, washed extensively with quartz distilled water, then immersed in 1 mg/ml poly-d-lysine (Sigma Chemical Co.) for 30 min at 25°C, rinsed with water, dried, then coated with Matrigel (Collaborative Research, Bedford, MA) for 30 min at 25°C, and thoroughly washed with $Ca^{++}$, $Mg^{++}$-free PBS. Generally, the coverslips were coated with Matrigel just before use. Neural tubes were plated at 19°C using a p200 Pipetteman pipetter by placing the tip just under the liquid surface before dispensing the neural tubes, and then allowing the neural tubes to settle by gravity. The cultures were ready for observation 5–8 h after plating. A few of the cultures were dissected using RTM dissecting media (12 mM NaCl, 4.0 mM KCl, 0.4 mM $Ca(NO_3)_2$, 0.05 mM $CaCl_2$, 0.8 mM Mg $SO_4$, 56 mM NaIsethionate, 4.0 mM $Na_2HPO_4$, 5.0 mM NaHEPES, pH 7.8, 0.1% Gentamycin) and plated in RTM media (20% Leibovitz L-15, 12 mM NaCl, 4.0 mM KCl, 0.4 mM $Ca(NO_3)_2$, 0.05 mM $CaCl_2$, 0.8 mM Mg $SO_4$, 56 mM NaIsethionate, 4.0 mM $Na_2HPO_4$, 5.0 mM NaHepes pH 7.8, 0.1% Gentamycin), supplemented with 1× embryo extract (Harris et al., 1985). The RTM media and the embryo extract increased the likelihood of finding flat neurons in the culture.

Just before observation, the cultures were placed in a custom-built chamber that was sealed under nitrogen. The chamber (illustrated in Fig. 1) consists of a thin (4 mm) metal base with a hole cut in the center to hold coverslips hinged to a thick (13 mm) top with a conically shaped well drilled into it. The coverslips are held between the bottom and the top using a silicone O-ring. A flat, plexiglass ring with a shallow well cut into it, was fitted to sit above the media, but within the well, as an open reservoir to hold oxygen scavenging solutions. In transferring the cultures from the petri dish to the cell chamber, the neurons would often lift off the coverslip from the surface tension of the liquid, which contained no serum. So, before transfer, a small amount of 5 mg/ml BSA in plating media was added directly over the explants to act as a surfactant. This was usually sufficient to prevent detachment of the neurons. Degassed media that had been bubbled with nitrogen was layered over the coverslip in the chamber, and the chamber was then placed in a nitrogen glove box. Under the nitrogen atmosphere, two separate oxygen-scavenging solutions, 1 M pyrogallol (Aldrich Chemical Co., Milwaukee, WI) in 1 N NaOH, and 0.4 M n-propylgallate (Sigma Chemical Co., St. Louis, MO) in 1 N NaOH were made fresh. 400 μl of each solution were placed in separate compartments of the open reservoirs described above. These oxygen scavengers helped to remove residual traces of oxygen in the chamber, and because they change color in response to oxygen, they indicated the presence of any leaks in the chamber. The chamber was then sealed air-tight using a clear plexiglass disc that covered the well and was held down by four thumbscrews.

### Microtubule Visualization and Data Acquisition

The neurons were visualized on an inverted microscope (Olympus IMT-2, Japan) equipped with epifluorescence optics, using the green filter set for rhodamine visualization and a 60×, 1.4 NA oil immersion objective. The light from the 100 W mercury lampsource was typically attenuated 4–10-fold with neutral density filters and constriction of an out of focus aperture. The excitation light was shuttered to 0.1 s per exposure. The frequency of image acquisition varied from 5 to 35 s, depending on the sequence. Images were collected using a Peltier cooled CCD camera (Photometrics Ltd., Tucson, AZ), equipped with a 900 × 900 pixel CCD chip (Texas Instruments, Dallas, TX). The final magnification onto the camera was 0.098 μm/pixel. For most experiments, only 512 × 512 pixels of information were collected. This allowed frequent image collection. Light shuttering and storage of digital data was controlled using a Microvax II workstation (Digital Equipment Corp., Marlboro, MA) coupled to a 32 Mgbyte Mercury Zip 3232+ array processor (Mercury Computer Systems Inc., Lowell, MA) and a display system (model 1280; Parallax Graphics Inc., Santa Clara, CA). The data was stored on a large format, 2 G-byte, optical disk (Emulex Corp./Optimem 1000, Costa Mesa, CA). This system was developed by Dr. David Agard and Dr. John Sedat. The images were photographed for publication using a Dunn digital camera system (Log E-Dunn) with Technical Pan 2415 film.

### Data Analysis

Microtubule growth and shrinkage measurements were performed on a Vax 8650 with an attached Parallax display station, using modelling and display software written in Fortran (Chen et al., 1989). The change in position of

the microtubule tips was measured for microtubules that were not moving laterally. The error in measurement was 0.1 μm based on repeated measurements of a microtubule. In a few cases, we measured the change in length between the tip of a microtubule and some static feature, such as a bend. An example of such a measurement is shown in Fig. 7, where a microtubule appears to shrink while it is simultaneously bending back toward the central region. The distance between the microtubule tip and a bend, which remains constant in shape, can be measured.

For clarity and detailed following of single microtubules (as seen in Fig. 8), some images of microtubules were traced by freehand from the video screen using modelling software (Chen et al., 1989).

The radius of gyration of the microtubules was determined by performing a line intensity scan across the growth cone in a direction perpendicular to the axon axis. A minimal cut-off intensity was determined for a single microtubules, and for each line intensity scan. This cut-off value was subtracted from all values, and any negative values were normalized to zero. The radius of gyration of the resulting distribution was determined with respect to the center of mass: $((\Sigma m_i r_i^2 - Ml^2)/M)^{1/2}$, where $m_i$ is the pixel intensity at a given position, $M$ is the total intensity across the line, $r_i$ is the distance of the pixel from the origin, and $l$ is the distance from the origin to the center of mass of the distribution. The width of the growth cone was determined from the same line intensity scans where a separate intensity cutoff was determined for the growth cone and the width of the resulting distribution was determined.

## Results

### Labeling Microtubules in Neurons

To label microtubules uniformly in neurons, we have developed a procedure in which labeled tubulin is injected into cells long before neuronal differentiation. The protocol for injection and neuronal culture is shown in Fig. 1. We injected rhodamine-labeled tubulin into *Xenopus* eggs during the first cleavage division and observed labeled microtubules 40 h later (at 18°C, 64 h at 13°C) in neurons explanted from the neural tube at the neurula stage. The embryo undergoes ~16 rounds of mitotic division to that stage, and generates 100,000 cells, but does not increase significantly in size. When the injected embryos were fixed and sectioned, or prepared as whole mounts, fluorescent tubulin could be easily seen in mitotic spindles and interphase asters throughout cleavage and gastrula stages (Reinsch, S. S., unpublished observations).

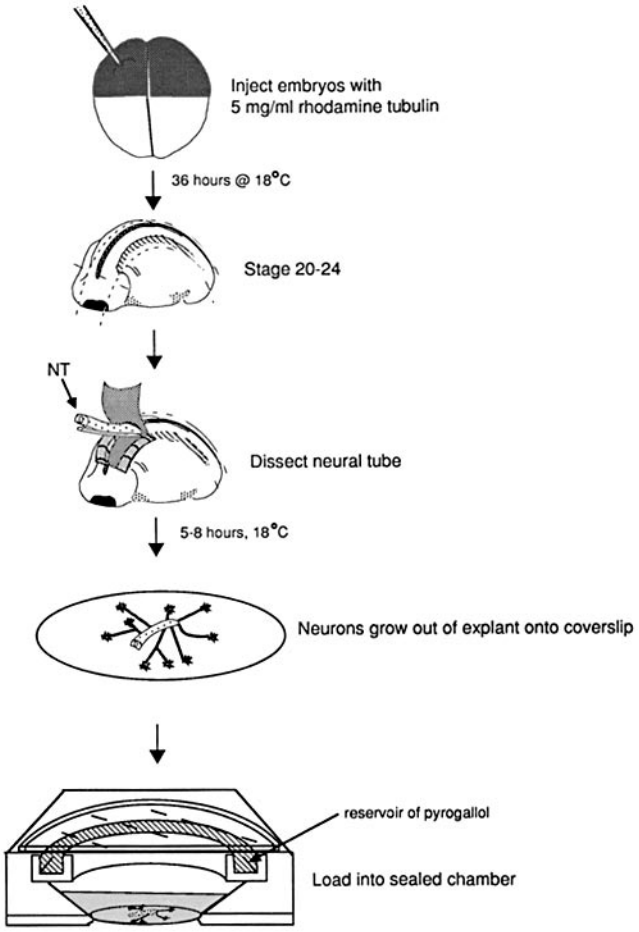


*Figure 1.* Outline of experimental procedure. Embryos are injected with 5 mg/ml rhodamine-tubulin at the two-cell stage. Neural tubes are dissected at stage 20–24, and plated as explants. Explants are viewed under anoxic conditions in a sealed chamber containing a reservoir of pyrogallol and n-propyl gallate.

To examine microtubules in neurons, we explanted small pieces of the neural tubes from normally developing embryos at ST 20–24 onto coverslips coated with a complex extracellular matrix. Fig. 2 shows a portion of an explant 5 h after plating, as neurons were beginning to emerge. The neurites had growth cones of various morphologies. In young cultures (4–10 h after plating), most growth cones had the classic features described for chick dorsal root ganglion and rat sympathetic neurons (Fig. 2, *inset*). They had significant regions of thin lamellipodia 5–10 μm in width with microspikes and filopodia emerging radially from the growth cone for distances up to 15 μm. Although most neurons generated straight axons, some branched or turned spontaneously. Axons grew out at rates of 70–250 μm/h at 19°C and reached lengths of several hundred microns. As the cultures aged (>12 h), the axons often developed varicosities and some of the growth cones started to become more bulbous, although they continued to grow. We concentrated our observations on the flat growth cones present in early cultures, because morphologically they resemble growth cones of well characterized neurons and because it was easier to visualize microtubules in thin flat regions of cells.

Under ambient conditions, overexposure to light (shuttered exposures more frequent than once every 15 s) caused growth cones to collapse, and the neurite to retract. During retraction, the microtubules and microtubule bundles became bent in response to the compression of the retracting growth cone and, as the microtubules bent, they appeared to twist around each other as they corkscrewed back toward the cell body. To reduce the cellular damage caused by singlet oxygen molecules generated during fluorophore excitation, the cultures were observed in a sealed chamber containing a reservoir of alkaline pyrogallol, to insure strict anoxic conditions throughout the experiment. Previous observations show that such explanted amphibian neurons can grow for several weeks in sealed chambers (Harrison, 1910). The removal of oxygen dramatically reduced photodamage and therefore increased the frequency of shuttered exposures (to every 5 s) that the cells could tolerate during fluorescence observation. The microtubules in the explanted neurons were imaged by epifluorescence optics and recorded digitally using a cooled charge-coupled device (CCD) camera.

### The Location of Microtubules in the Growth Cone

We will first describe the static images of microtubules in these neurons and then analyze properties of their distributions that could only be appreciated by time-lapse observa-

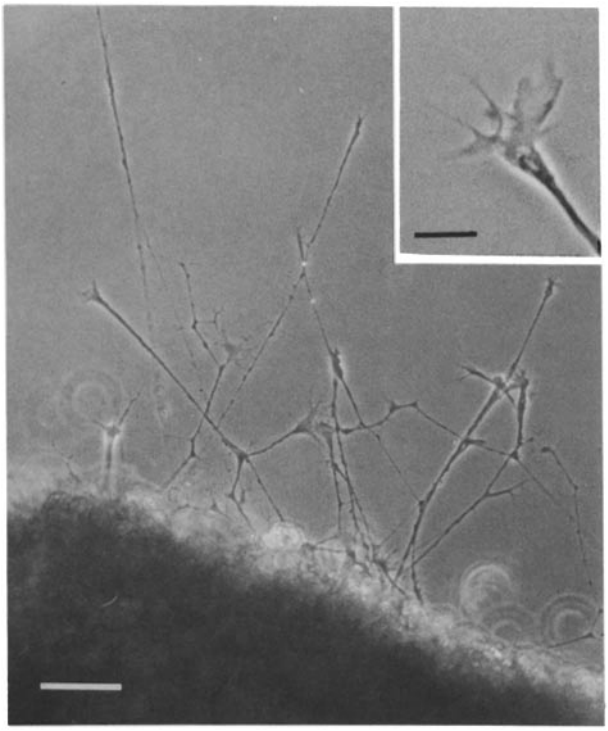

*Figure 2.* Low magnification phase image showing approximately one fifth of a typical neural tube explant, 5 h after plating. The cell bodies remain in the neural tube (lower portion of micrograph) as the neurites emerge. Later, additional neurons will grow out. (*inset*) High magnification view of one growth cone from the explant. Bars: (*lower portion of micrograph*) 50 μm; (*inset*) 8 μm.

tions at a level where single microtubules could be resolved. In growth cones, especially at their periphery, it was possible to distinguish single microtubules; in the most favorable cases we could describe in detail the distribution of microtubules in the entire growth cone. We recorded the microtubule distributions in 52 neurons in 24 experiments. In almost every instance we found that appreciable numbers of microtubules extended beyond the growth cone neck, deep into the peripheral lamella where they frequently touched or closely approached the membrane (Fig. 3, *A* and *B*, *arrows*). While individual microtubules in the lamella could be resolved, most of those in the central region were so closely packed that they could not be resolved. Organelle accumulations recorded by phase microscopy (Fig. 3, *A*, *C*, and *E*), corresponded roughly, but not precisely, to the regions of highest microtubule density; they are probably identical to the "organelle-rich regions" described in Aplysia neurons using Nomarski optics (Goldberg and Burmeister, 1986). Microtubules were not limited to these regions of high organelle density; for example, in Fig. 3, *A* and *B*, a small bundle of microtubules extended well beyond the dense organelle region (Fig. 3, *arrowheads*). Therefore, the use of organelle location to denote microtubule location may not always be justified.

The total number and distribution of microtubules in growth cones varied dramatically among different neurons. In some neurons, it was possible to resolve almost all of the microtubules, while in others, the thick tangle or close packing of microtubules in the central region made counting impossible. Our best estimate is that the number of microtubules per growth cone ranges from 10 to 40, and this number is roughly proportional to the size of the growth cone.

We could group the microtubule distributions into three general classes. A corresponding phase and fluorescence image of a typical growth cone from each class is shown in Fig. 3. In the first class, microtubules penetrated most of the projected growth cone area as seen in Fig. 3 (*A* and *B*). Many of the microtubules were bent or sinuous and were somewhat dispersed, even in the central region. We will refer to this distribution as the splayed distribution. In the second class, as seen in Fig. 3 (*C* and *D*), microtubules were also bent and spread, but they were not sinuous; rather, they formed loops that had a small radius of curvature. In such neurons, it was not uncommon to see microtubules that were bent by 90° or more. Such bending caused the distal ends of growth cone microtubules to be perpendicular to the direction of the axon bundle. We will refer to this configuration as looped. In the third category of growth cones (Fig. 3, *E* and *F*), almost all of the microtubules were straight, and even deep in the growth cone the width of the array did not deviate considerably from the width of the axon bundle. Sometimes, in this distribution, small bundles were resolvable whereas at other times, the array appeared to be of uniform brightness. This distribution, which we call bundled, left large regions of the growth cone unoccupied by microtubules (Fig. 3, *E* and *F*, *arrows*) with single microtubules occasionally straying from the main bundle (Fig. 3, *arrowhead*). In all three classes of neurons, microtubules extended to distal portions of the growth cone. Such diverse morphologies could represent distinct populations of neurons. However, when individual neurons were followed over time, as we discuss below, we observed an interconversion of the microtubule arrays among the splayed, looped, and bundled configurations.

## *The Origin of Microtubules in the Growth Cone*

***Microtubule Dynamics.*** Assembly of tubulin at steady state can be characterized by four parameters: the polymerization rate, the depolymerization rate, the rescue rate (shrinking to

*Figure 3.* Phase and fluorescence images of three living *Xenopus* neurons showing the three classes of microtubule distributions. (*A* and *B*) Phase and fluorescence images of a growth cone with a splayed microtubule distribution. Images were taken 44 s apart. Microtubules penetrate into the edges of the lamella in two places, shown by arrows. Arrowheads indicate areas where microtubules or small microtubule bundles extend beyond organelles. (*C* and *D*) Phase and fluorescence images taken 5 s apart, of a growth cone with a looped microtubule distribution. Microtubules penetrate to the edges of the growth cone. Many of the microtubules form acute bends which cause their distal ends to be perpendicular to the direction of the axon. (*E* and *F*) Images of growth cone with a bundled distribution taken 13 s apart. Microtubules in this growth cone are predominantly straight, and remain in a coherent axon-like bundle deep into the growth cone. Significant regions of the growth cone are left devoid of microtubules (*arrows*). A single microtubule is observed to form a loop near the neck (*arrowhead*). Bar, 5 μm.

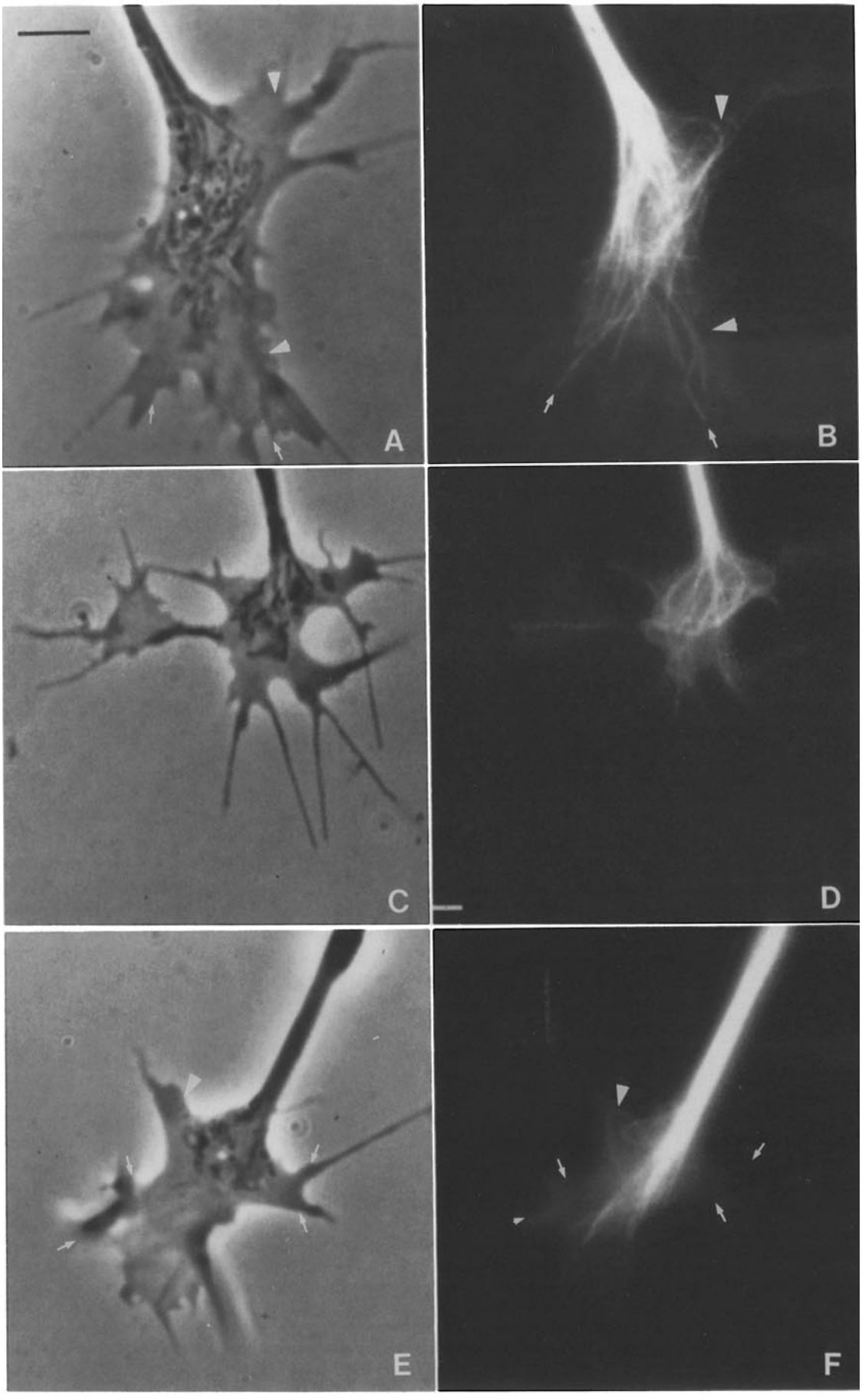
A
B
C
D
E
F

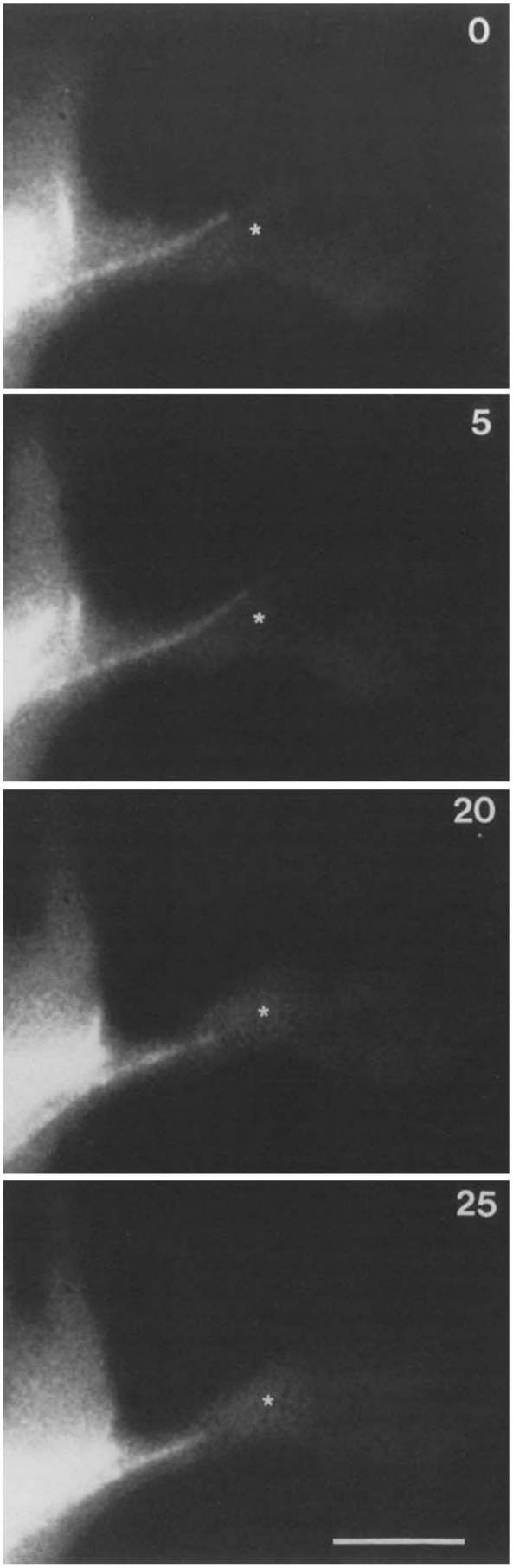


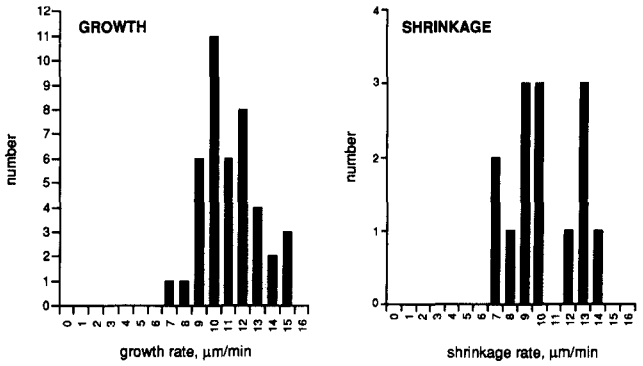


*Figure 5.* Histogram of growth and shrinkage rates. The movements of microtubule tips were measured (microtubules that simultaneously underwent lateral translocation were not included). Each measurement represents the measurement of a single tip between two frames. Measurements on the same microtubule at different times were considered independent measurements, as these rates varied considerably. Mean growth rate and SD, 10.6 ± 1.91 μm/min. Mean shrinkage rate, 9.7 ± 2.28 μm/min.

growing transition), and the catastrophe rate (growing to shrinking transition). To measure these assembly rates in growth cones, we acquired images of microtubules every 5–10 s in six cells. In general, we observed that isolated microtubules in peripheral areas had clear periods of sustained growth followed by sustained shrinkage (Fig. 4). For microtubules that showed little lateral movement, it was possible to measure with precision the change in the position of the microtubule end, as a means of measuring growth and shrinkage. In this way, we could measure the dynamics of 20–40% of the microtubules in these growth cones; the majority resided in densely populated regions of the growth cone where lateral motions and the high density of microtubules prevented accurate measurements. The mean growth rate for 42 measurements in the six neurons (Fig. 5) was 10.6 (SD 1.9) μm/min, while the mean shrinkage rate was 9.7 (SD 2.28) μm/min ($n$ = 14) (Fig. 5). Some microtubules did not appear to grow or shrink between two frames, as their tips remained stationary. We estimate that 15% of the microtubules whose tips we could follow were in this category.

The catastrophe rate was calculated as described previously (Walker et al., 1988; Belmont et al., 1990). We followed microtubules that could be discerned to be growing, and summed the total amount of time spent in growth for all of the microtubules. (This included microtubules that were growing and were subsequently lost from view.) This total time was then divided by the total number of transitions to shrinkage observed for these microtubules. Of 33 growing microtubules observed (1,560 s of growth), 18 were observed to shrink while 15 were lost. From these observations, we calculated a transition frequency of 0.72 $min^{-1}$. We could not measure rescue frequencies reliably, primarily because the region in which isolated microtubules are observable in

*Figure 4.* Growth and transition to shrinkage of a microtubule at a growth cone periphery. Microtubule extends 1.0 μm between 0 and 5 s, and recedes 1.9 μm between 5 and 20 s. The asterisk marks a constant position in the field. Bar, 5 μm.

*Table I. Comparison of Microtubule Dynamics in Growth Cones with Those in Non-neuronal Cells and in Cell Extracts*

| Cell type | Growth | Shrinkage | Catastrophe | Rescue |
|---|---|---|---|---|
| | *μm/min* (± SD) | *μm/min* (± SD) | $s^{-1}$ | $s^{-1}$ |
| Xenopus neurons | 10.5 ± 1.9 | 9.7 ± 2.2 | 0.012* | – |
| Xenopus extract (interphase)§ | 9.3 ± 4 | 12.8 ± 6.0 | 0.01-0.031* | 0.009-0.016* |
| BSC-1 fibroblasts‖ | 5.0 ± 2.4 | 7.4 ± 2.7 | – | – |
| Newt lung epithelia¶ | 7.2 ± 1.9 | 17.3 ± 4.1 | 0.014‡ | 0.044‡ |
| Human fibroblasts** | 3.5 ± 3.2 | 4.3 ± 5.7 | – | – |

* Determined as described in Walker et al. (1988).
‡ Determined as described in Cassimeris et al. (1988).
§ Belmont et al. (1990).
‖ Schulze and Kirschner (1988).
¶ Cassimeris et al. (1988).
** Sammak and Borisy (1988).

the lamella was very limited (≤12 μm), so shrinking microtubules were lost in the dense population of microtubules in the central region.

Such measurements do not distinguish growth or shrinkage at the distal end from the forward or backward translocation of stable polymer. We believe that at least some of the measurements represent actual polymerization and depolymerization for several reasons, none of which completely excludes microtubule translocation. First, both growth and shrinkage rates resemble rates found in other systems (Table I), and are especially close to rates found in *Xenopus* egg extracts. Second, 55% of the microtubules could be observed to transit from growing to shrinking. It seems less likely that translocating microtubules would change direction abruptly. Third, in some cases, we observed the change in length between the tip of a microtubule and some static feature, such as a bend. An example of such an event is shown in Fig. 7. The larger arrows follow the tips of two microtubules, while the smaller arrows mark the position of bends in these microtubules. In the upper microtubule, the distance between the microtubule tip and the bend increased between 5 and 35 s, while for the lower microtubule, the distance decreased between 10 and 25 s. Again, we believe that this type of behavior is more likely to be due to growth and shrinkage, rather than the translocation of a polymer through a sinuous track.

***Microtubule Translocation.*** New microtubule polymer in the growth cone also appeared to be generated by mechanisms other than polymerization. We have consistently observed what we interpret to be bulk sliding of microtubules from the axon into the growth cone. For single microtubules, this is an impression that would be difficult to prove without some marking on the microtubule that could distinguish translocation from polymerization off the free distal end. Bulk sliding was most clear when we observed the simultaneous movement of groups of microtubules. Loops consisting of several microtubules often maintained a stable configuration, and yet were translocated forward as a group within the growth cone. Loops in different regions of the growth cone moved at the same time, and approximately at the same rate. Fig. 6 shows such a translocation event. Within the 30-s sequence, though the morphology and position of the growth cone did not change relative to the substrate, there was a forward translocation of microtubule loops which maintained a coherent structure into the growth cone. The upper and lower arrows point to stable morphological features on the loops of microtubules, while the smaller arrows mark a constant position in the field; loops on both sides of the growth cone moved at the same time. The upper loop translocated 2 μm in 20 s while the lower loop translocated 1.6 μm during this time.

### *The Generation of Splayed, Looped, and Bundled Microtubule Configurations in the Growth Cone*

The most striking property of microtubules in growth cones were the forward and lateral translocations as well as bending movements that resulted in rapid changes in the overall distribution of microtubules in the growth cone. We have attempted to understand the cause of these movements and how they generate large-scale changes in the microtubule distribution, and finally, how these changing microtubule configurations are related to growth cone behavior and axon elongation. We analyzed in detail the microtubule distributions in 12 neurons over times ranging from 4 to 30 min. Phase images were not usually acquired during these sequences, but the signal generated from the fluorescence of tubulin monomer was used to define the edges of the cell, as can be seen in Fig. 2.

***Microtubule Splaying.*** When the microtubules in the growth cone were in the splayed configuration, the growth and shrinkage of microtubule ends was most easily visualized. We often observed that single microtubules that grew relatively straight into the lamella became bent or moved laterally. This resulted in the formation of wavy microtubules that would eventually shrink back to the central region. As in other cell types, the individual microtubules appeared to behave independently. Fig. 7 shows an example of such behavior. A single microtubule that extended rather straight into the periphery, as indicated by the lower arrow at 0 s, began to bend at 5 s (Fig. 7, *lower small arrow*). The bending continued through 20 s and the length from the microtubule tip to the bend shortened until the tip was barely visible at 35 s. The microtubule indicated by the upper arrow at 0 s also bent during the sequence (Fig. 7, *upper small arrow*), but its end lengthened with respect to the bend.

***Looping.*** During the generation of the looped configuration, we observed the formation of acute bends in many microtubules. Fig. 8 follows the formation of a looped structure. At 0 s, a single microtubule (Fig. 8, redrawn in the *right*

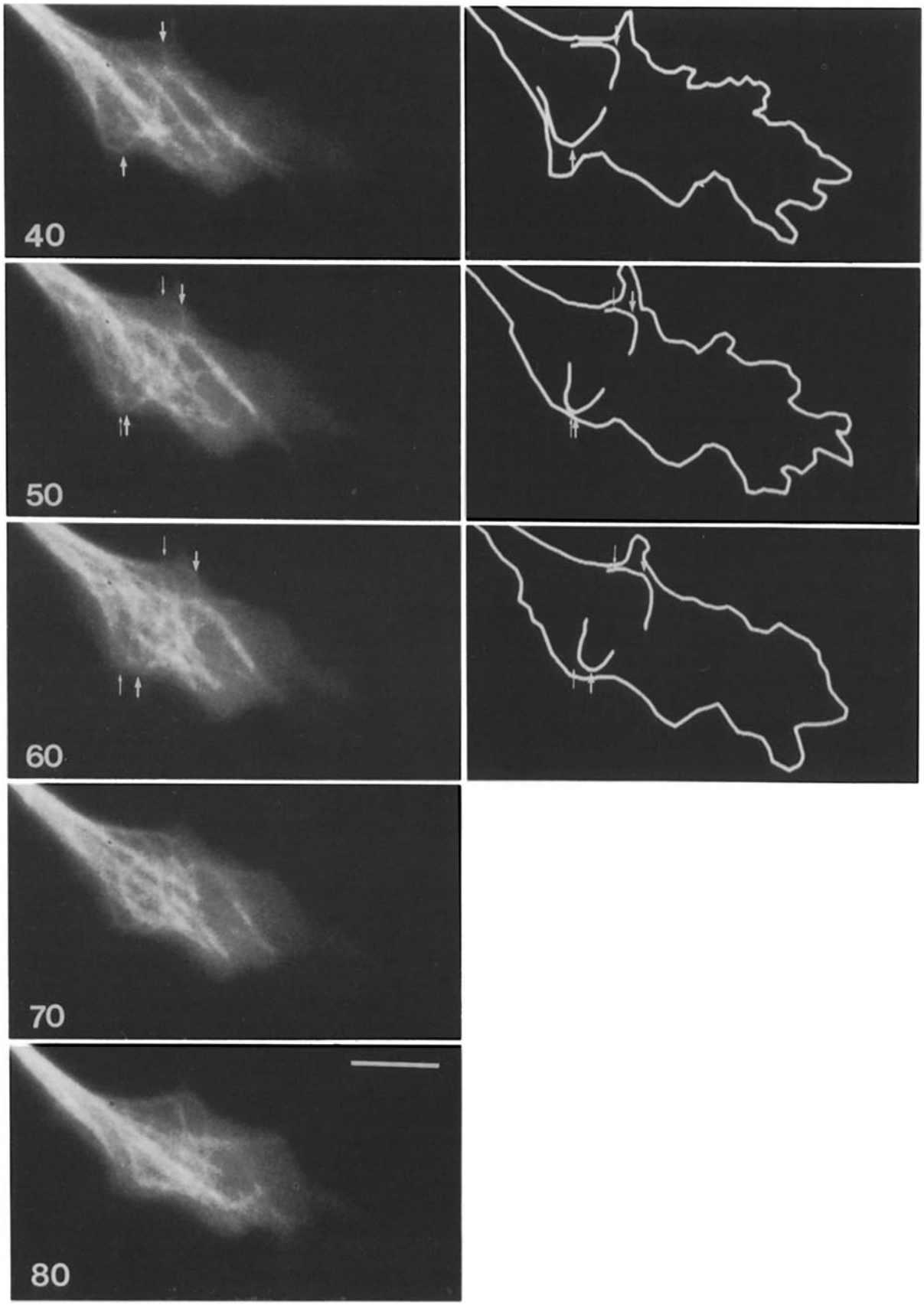


*Figure 6.* Forward translocation of microtubule loops in the growth cone. Larger arrows follow similar points on the microtubules (based on morphological criteria), while small arrows mark constant positions on the field (the positions of the arrows at 40 s). The upper loop moved forward 2.0 $\mu$m between 40 and 60 s, and the lower loop moved 1.6 $\mu$m within the growth cone, while the morphology and position of the growth cone is constant. The microtubules followed by the arrows and the outline of the growth cone have been redrawn on the right panel for clarity. Bar, 5 $\mu$m.

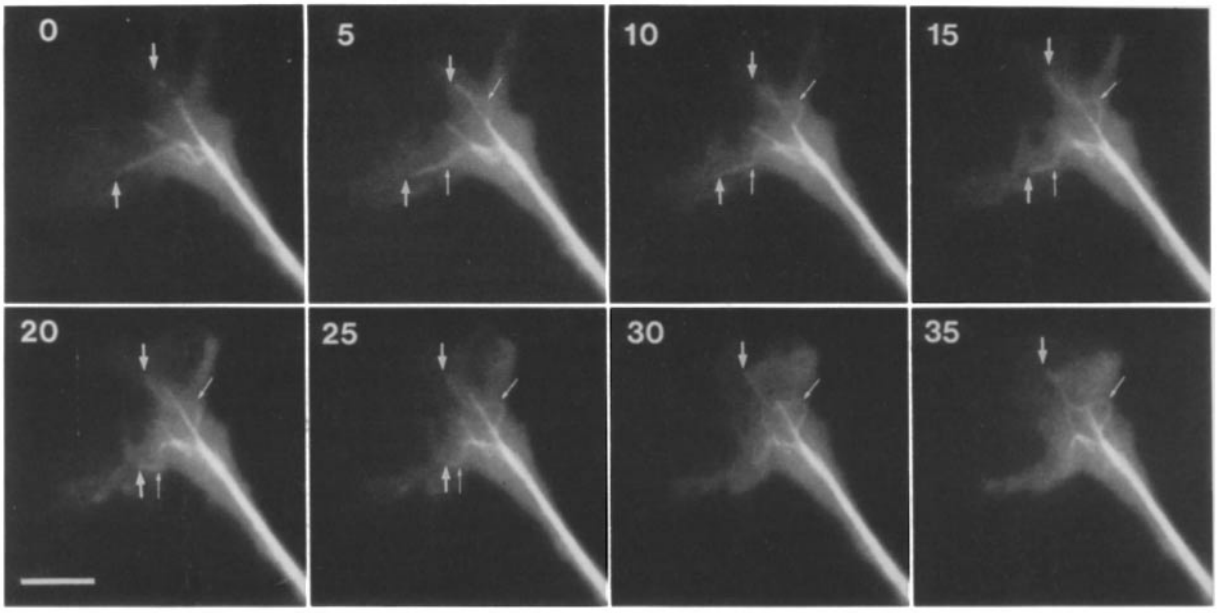


*Figure 7.* Bending of single microtubules in the peripheral regions of the growth cone. At time zero, two microtubules in the periphery (indicated by *larger arrows*) are relatively straight. Both microtubules form bends (marked by *smaller arrows*) at 5 through 15 s. For the upper microtubule, the length between the tip and the bend increases between 15 to 35 s. For the lower microtubule, the distance between the microtubule tip and the bend decreases during the same time. Bar, 5 μm.

*panel*) was quite contorted, making three bends, but most of the other microtubules were slightly spread, and pointed in the general direction of the axon. At 10 through 30 s, the bending of the redrawn microtubule became more acute, while the other microtubules began to bow out. By 40 and 50 s, multiple microtubules formed acute bends so that by 50 s, the distal ends of the microtubules looped back towards the axon rather than pointing out to the growth cone periphery.

Several forces could potentially have caused such microtubule bending and looping. First, the ends of the microtubules could have been pushed backward toward the axon; as a consequence, the sides of the microtubule would have bowed out. Second, the microtubules could have polymerized at their distal ends while in contact with a fixed barrier, resulting in increased microtubule length and in this constrained situation, buckling of the microtubule. Third, the microtubules could have been translocated forward into the growth cone against a fixed barrier. This forward translocation would have resulted in a compressive force on the microtubules that could have caused bending and buckling.

When single microtubules in the growth cone periphery became bent, as seen in Fig. 7, it was difficult to distinguish between these types of forces without a fiduciary mark on the microtubule. However, during the formation of looped configurations, the increase in the contour length of microtubules in the growth cone along with the forward movement of looped structures suggested that the formation of loops in the central region occurred primarily through the forward translocation and compression of microtubules. This can clearly be seen in the single microtubule that has been redrawn by in the right panel of Fig. 8. At 0 and 10 s, the contour length of the microtubule between two points that were fixed with respect to the substratum (Fig. 8, indicated by the *arrowhead* and the *arrow, right panel*) increased from 13.5 to 15.1 μm, while the tip of the microtubule moved forward ~0.7 μm. This could be due either to growth at the tips of the microtubule in the presence of a barrier and consequent buckling or to the translocation of polymer against a barrier and subsequent buckling. However, between 20 and 50 s the loop marked by the asterisk moved forward with respect to the substratum by 3.6 μm. It is unlikely that distal polymerization would cause the loop close to the neck to move forward in space.

***Bundling.*** During the formation of looped structures, there was an increase in the microtubule contour length in the growth cone, and the arrangement of the microtubules which were apparently under compressive forces, became more compact (Fig. 8). These highly contorted configurations were not stable endpoints; within a few minutes microtubules underwent a restructuring to form axon-like bundles within the growth cone. Fig. 9 shows an example where the looped arrangements of the microtubules rearranged into an axonal bundle. Previous to the time points shown, over a period from 0 to 175 s (relative to Fig. 9), we observed that the microtubules in the growth cone formed tight loops so that the distal ends of the microtubules pointed perpendicularly to the direction of the axon, with no microtubules pointing into the periphery. Measurements of microtubule contour length and of the forward translocation of loops, again, indicated that these loops had formed via buckling in response to forward translocation of polymer. By the first time point shown in Fig. 9 (280 s), these microtubules had begun to unfold so that they appeared partly splayed and partly looped. After 280 s, they continued to gradually straighten, so that at 315 and 350 s, microtubule ends entered the peripheral regions of the grow cone. By 385–455 s, the radius of curvature of the microtubules had decreased considerably, until at 490 and 525 s the microtubules, particularly in the proximal portion of the growth cone, coalesced to form the newest part of the axon.

During the formation of bundles in the growth cone, in ad-

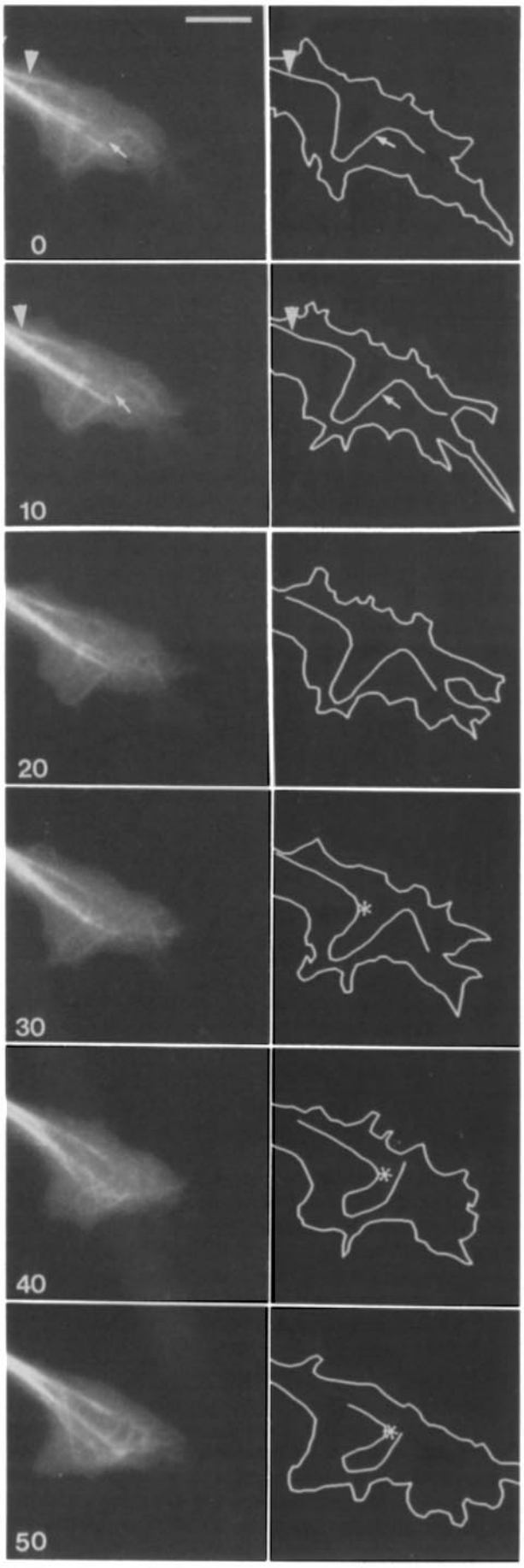


dition to the unfolding of compressed, looped microtubules, we also observed the extension of a microtubule bundle that had already formed in the growth cone. It is not known whether these microtubules grew by polymerization, or whether they emerged by sliding and translocation. In Fig. 10, three microtubules were seen to extend from the distal end of a bundle. At 0 s, three microtubule tips that emanated from the main microtubule bundle were barely discernable. From 15 to 45 s, these tips emerged from the bundle at rates of 8.9 μm/min (Fig. 10, *left microtubule*), 12.1 μm/min (Fig. 10, *center microtubule*), and 10.0 μm/min (Fig. 10, *right microtubule*). In contrast to the microtubules in Fig. 7, these microtubules pointed in the same direction as the microtubule bundle, and remained straight.

The conversion of bent (splayed or looped) microtubules and small microtubule bundles into larger, straight bundles was observed in five out of eight neurons. One of the five underwent three rounds of bending and straightening in 50 min with intervals of 330 and 297 s between bundling events. Of the remaining three growth cones, one (depicted in Fig. 7) had splayed microtubules that shrank back to the central bundle of microtubules. This was followed by the emergence of several microtubules from the bundle and subsequent elongation. One neuron maintained a looped microtubule array throughout the 50-min period of observation, while another displayed a splayed distribution throughout a rather short period of observation (4 min). The four neurons that branched or turned were not included in these classifications, though they too displayed episodes of bundling and splaying.

### *Microtubule Bundling and Growth Cone Advance*

Ultimately, the generation of new axon requires both the collapse and quiescence of the actin rich cortex and the bundling of microtubules. Thus, the finding that bundling occurred in the growth cone and often accompanied growth cone advance may simply reflect a passive response of the microtubules to a constriction of the plasma membrane generated by the actin cortex. If this were the case, we would expect that bundling would accompany collapse of the membrane. However, in several cases, we observed that microtubules that were looped or splayed, clearly formed bundles within the growth cone before the collapse of the growth cone membrane, and subsequent formation of new axon. Fig. 11 shows a growth cone that exhibited bundling before the collapse of the growth cone membrane. (Although images were acquired at 10-s intervals, here, we have only included images at 30-s intervals.) Bent microtubules accumulated in the first 60 s of the sequence mainly by translocation of loops into the growth cone. Between 60 and 90 s, the width of the

*Figure 8.* Forward translocation and looping of a single microtubule in the growth cone. The growth cone and a selected microtubule are redrawn in the right panel. The outline of the neurons looks larger than the diffuse fluorescence because it was not possible to reproduce all of the gray scales in the original image. Between 0 and 10 s, the contour length of the microtubule between the points marked by the arrowhead and the arrow (fixed with respect to the field) increases from 13.5 to 15.1 μm. The tip of the same microtubule moved forward 0.7 μm. Between 20 and 50 s, the microtubule loop marked by the asterisk moves forward 3.6 μm. Bar, 5 μm.

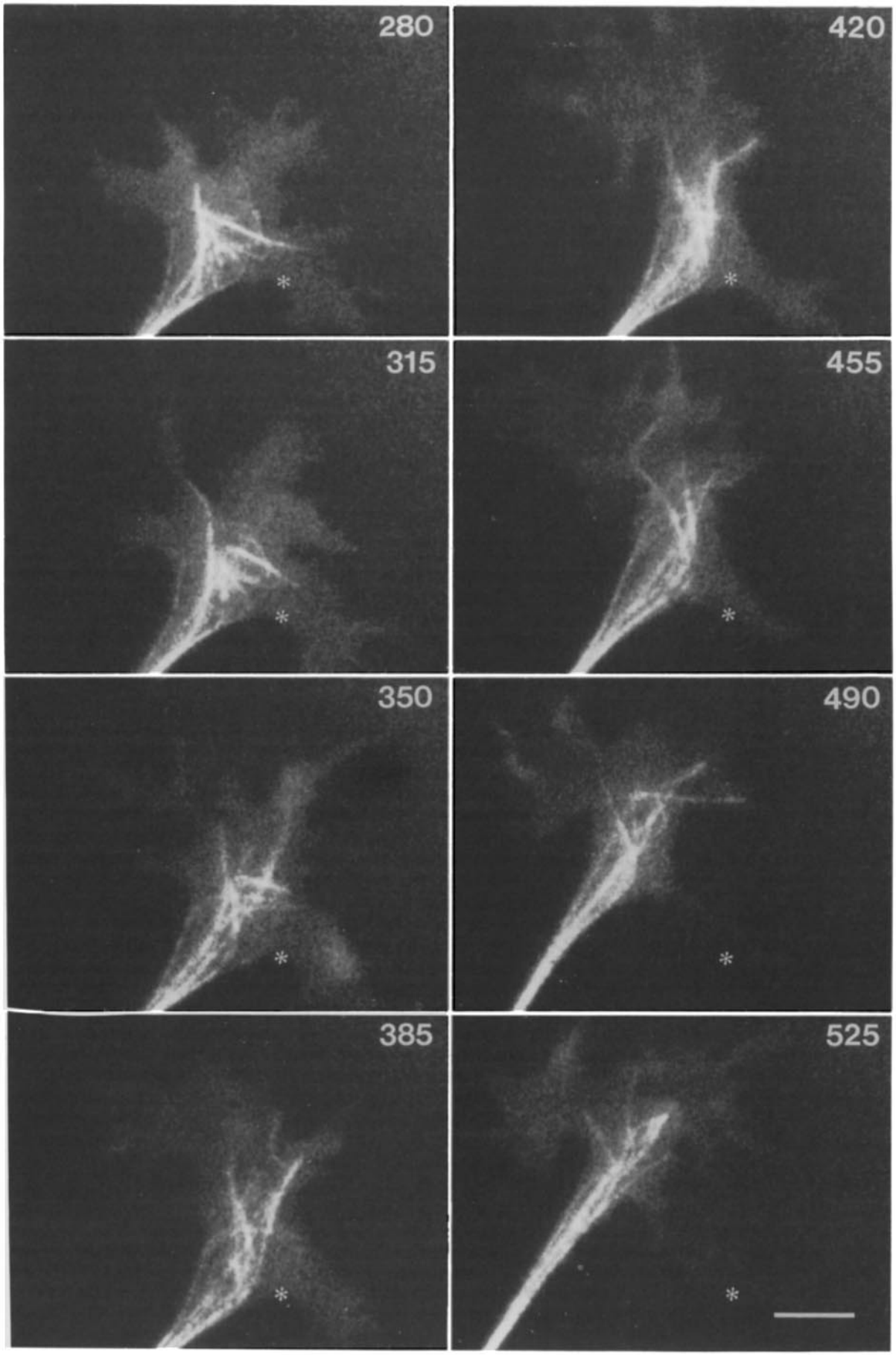


*Figure 9.* Straightening and bundling of microtubules in the growth cone during axon formation. Microtubules are contorted at 280 s. Between 315 and 525 s, they gradually straighten, and by 525 s, form part of the new axon. The microtubule bundles coalesce before the lamellar region on the right collapses between 455 and 525 s. Asterisk marks a constant position on the field. Bar, 5 $\mu$m.

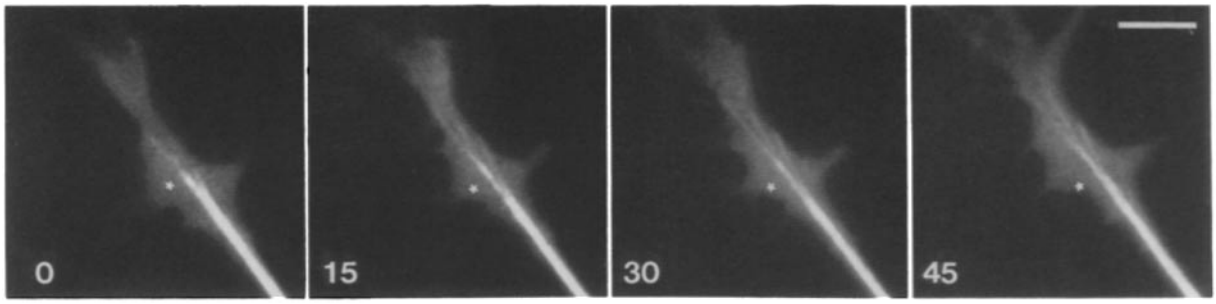


*Figure 10.* The extension of a microtubule bundle in the growth cone. Three microtubules simultaneously emerge from the end of the main axon bundle. These microtubules do not bend or deviate considerably from the main course of the bundle. Asterisk marks a constant position in the field. Bar, 5 μm.

growth cone did not change significantly but the microtubule array in the proximal region of the growth cone began to bundle. By 120 s, the width of the microtubule array in the proximal region of the growth cone closely resembled that in the axon, and by 180 s, the microtubules in the distal region of the growth cone also became restricted while a large lamellipodia extended forward. At 210 s, the proximal membrane collapsed around the microtubule bundle and a lamellipodia extended forward while the microtubules in the growth cone began to spread and loop. A second round of microtubule looping in the growth cone occurred between 210 and 300 s.

To assay bundling and membrane distribution quantitatively, we measured the diameter of the growth cone across a line that was fixed with respect to the field (the endpoints of the line are indicated by *arrows* in Fig. 11). This was correlated with the lateral distribution of microtubules along this line as measured by the radius of gyration of the microtubules on the line. The radius of gyration is a weighted measure of the radial distribution of the microtubules from the center of mass (see Materials and Methods for precise calculation). A plot of these parameters for the growth cone in Fig. 11 is shown in Fig. 12. Both the width of the growth cone and the radius of gyration of the microtubules were large in the early sections and both decreased as the growth cone advanced, and transformed into axon. The start of microtubule bundling (Fig. 12, *arrow A*) preceded by 20 s the beginning of the decrease in the width of the growth cone cortex (Fig. 12, *arrow B*). When we examined nine periods of rapid growth during which microtubules became bundled to form new axon, the initiation of microtubule bundling preceded growth cone collapse in four (for example, Fig. 11 at 180 s). In four, bundling and membrane collapse occurred so close together that they could not be distinguished. In one, the bundling had already occurred before the beginning of the sequence.

### *Microtubule Placement during Growth Cone Turning*

During our study of growing axons, we observed a few neurons that spontaneously made sharp turns, and one that branched. Though it is not our purpose to study turning in detail here, it was of particular interest to learn whether microtubules were oriented within the growth cone during turning, and, if so, whether similar mechanisms of microtubule translocation and bundling were used in the orientation of microtubules during turning. Of four growth cones that turned or branched, one had clearly begun to turn before observation began, but in the other three cases the morphology of the growth cones initially looked quite symmetrical and there was no indication to us that the growth cone would turn. When we examined the microtubules in these three growth cones, we found that several microtubules, but not all, were already oriented in the direction of future growth. For example, in Fig. 13, at 0 s, the growth cone had three large lamellipodial expansions, to the right, toward the center (Fig. 13, *arrowheads*), and to the left; the future direction of its course as judged by its cortical morphology was ambiguous. However, there was a slight asymmetry in the microtubule distribution, several microtubules curved gently to the right with a single microtubule protruding slightly into the right lamella, none entered the center, and only a few entered the left lamella. Because these microtubules were oriented before observation began, we do not know how they became oriented. Microtubules that subsequently entered the growth cone from the axon bundle were routed primarily to the right when they contacted the upper cortex. The small arrow at 10 through 45 s indicates microtubules as they initially extended straight into the growth cone. When they contacted the upper membrane they bent to the right. This bending resembled the bending observed during formation of the microtubule loops during forward growth. Whereas in looping, the microtubules bent back toward the center of the growth cone (as seen in Fig. 8) and crossed each other; during branching, the microtubules bent outward, and during turning, most microtubules bent in one direction. As in forward growth, we then observed the formation of microtubule bundles within the growth cone in the direction of growth. In Fig. 13, the pro-

*Figure 11.* Sequence of microtubule bending and bundling during outgrowth. In the first three frames, microtubules emerging from the neck bow out and fill most of the area of the growth cone. Many bent microtubules are observed in the central region. At 90 to 180 s, microtubules become extended and coalesce into a bundle within the growth cone. The formation of microtubule bundles precedes the collapse of membrane at the neck. Frames 210 to 300 show the recurrence of microtubule bending. The growth cone moves 15 μm in 300 s. The arrows indicate the endpoints of the line on which pixel intensity was measured for the radius of gyration measurement. Bar, 5 μm.

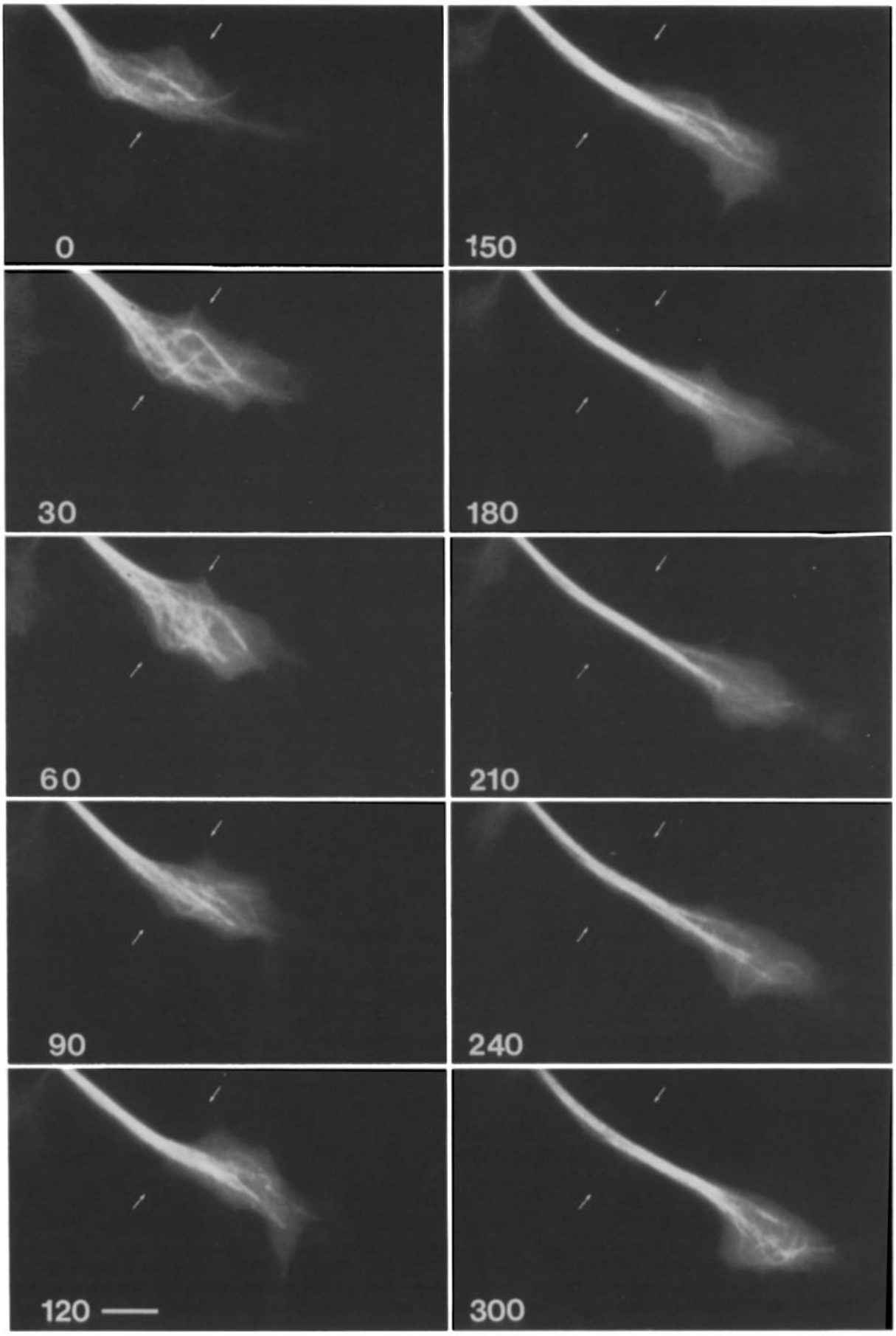
0
150
30
180
60
210
90
240
120
300

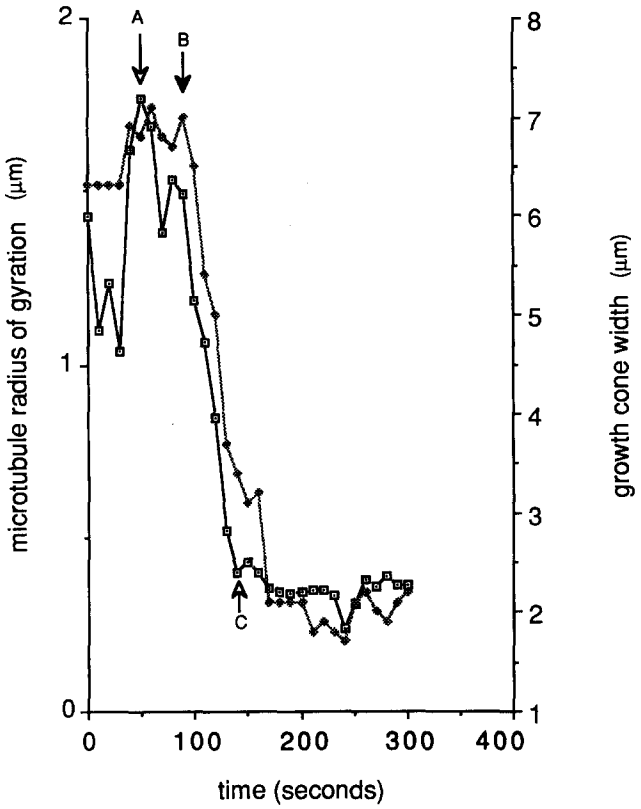


*Figure 12.* Comparison of the microtubule radius of gyration and the growth cone width along a constant line perpendicular to the axon for the growth cone in Fig. 11. (*open squares*) Microtubule radius of gyration. (*closed circles*) Growth cone width. The microtubules begin to bundle (as marked by *arrow A*) 20 s before the growth cone begins to collapse (*arrow B*). At 120 s (*arrow C*), the microtubules are bundled, while the growth cone has not completely collapsed.

gressive bundling of microtubules occurred between 55 and 185 s, well before the growth cone began to collapse to form the axon. The initiation of bundle formation before the collapse of the growth cone was observed in two neurons, while in the other two cases, the events occurred too close together to distinguish.

In two of the turning growth cones, microtubules that were not oriented in the future direction of growth were present and were seen to persist, even after the future direction of growth was quite clear. In Fig. 13, several microtubules occupied the left lamella from 0 s, and although the orientation of the axon bundle was clear by 55 s, a single microtubule persisted until 155 s. This microtubule, rather than shrinking back into the bundle, was zippered into the forming bundle. The arrows at 115 and 155 s follow the end of the microtubule, while the arrowheads (115, 155, and 185 s) follow the proximal region as it is dragged to the right and joins the bundle, forming an acute bend in the region where the microtubule joins the bundle (Fig. 13, *arrowheads*, 185 s). This leaves the left lamella unoccupied by any microtubules at 185 s.

## Discussion

The ability to observe microtubules in living cells offers several advantages over the use of fixed specimens. First, it avoids the potential artifacts due to fixation. Microtubules are difficult objects to preserve and recent knowledge of their dynamics provides an explanation for the early difficulties. (If a fixation process in a cell takes 10 s, a microtubule in this time can lose 50,000 subunits and shrink by 3 μm.) More importantly, by observing living cells we can describe microtubules as they grow and move, and in this way describe the process of generating new structures within the cell. These dynamic changes in microtubules can then be compared to other dynamic behaviors of the cell. In this report, we have examined the dynamic changes of microtubules within growth cones and correlated these changes with events involved in axon extension.

### The Location of Microtubules in the Growth Cone

Although microtubules were consistently found to extend deep into the periphery of the growth cone, the overall arrangement of microtubules was variable. We have grouped these distributions into three general categories: splayed, looped, and bundled. Although there were many times where the distribution exactly fit in a single category, intermediate distributions existed in which characteristics of two types were often seen. Thus, these categories are merely archetypes and do not reflect the existence of discrete states.

Similar variations in distribution have been described previously. The splayed configuration, in which microtubules extend and diverge into the periphery has been described by electron microscopy for chick retinal neurons (Cheng and Reese, 1985), and in rat superior cervical ganglion neurons using EM and immunofluorescence (Bridgman and Dailey, 1989). The looped distribution, in which microtubules loop backwards and form sharp bends, as well as the splayed distribution, have been seen by both Tsui et al. (1984) and Lankford and Klein (1990) in chick retinal cells. These two distributions have now been seen in living grasshopper pioneer neurons at the light level and in fixed specimens using EM (Sabry et al., 1991). Because previous analyses were limited to fixed cells, it was not clear whether these distributions were stable features of particular types of neurons or whether they were temporary features related to the activity of the nerve cell.

An important conclusion from our work is that the

*Figure 13.* Sequence of microtubule collapse and bundling as a neuron begins to turn. At zero seconds, the microtubules are already oriented to the left and to the right, even though a large lamella points along the central growth cone axis (*arrowheads*). Single microtubules, indicated by arrows, emerge from the central region of the growth cone (10, 20, 25). These microtubules extend into the periphery of the growth cone and bend to the right as the edge of the cell also collapses in this region. Subsequently (55–105), the dispersed microtubules become bundled toward the right. A single microtubule remaining in the left side of the growth cone retracts, leaving the left lamella without microtubules. At 115 through 155 s, the arrowheads follow the proximal portion of the single microtubule that remains in the left lamella, but is then zippered into the main bundle.

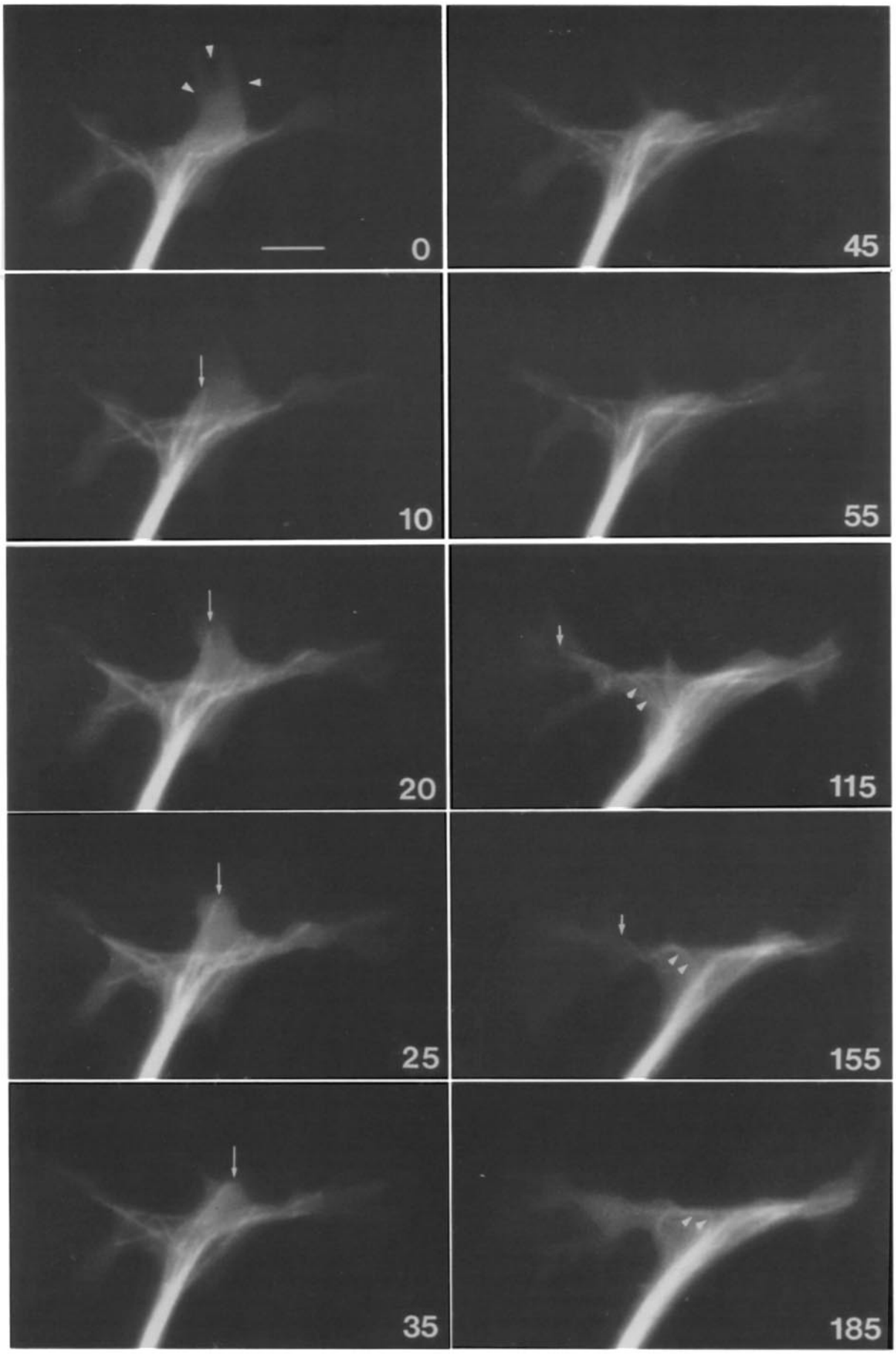
0
45
10
55
20
115
25
155
35
185

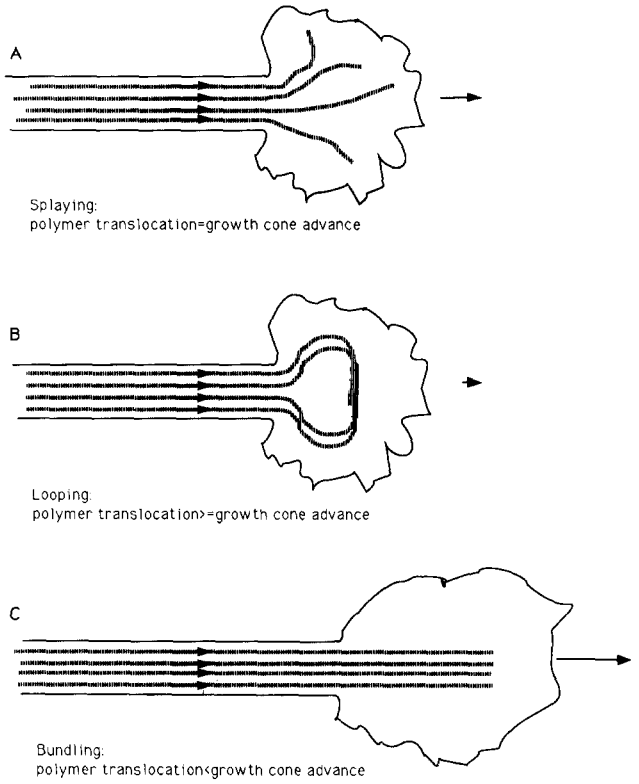


*Figure 14.* A schematized representation of the relationship between microtubule translocation and growth cone advance. The arrows superimposed on the microtubules represent the rate of translocation of the microtubules, while the arrows at the leading edges of the growth cones represent the rate of advance of the growth cone. For each growth cone, the relative rates of the microtubules and the growth cone are related to the configuration of the microtubules inside of the growth cone.

microtubules in a single neuron can alternate rapidly between these configurations during growth cone extension. We find that any of the three distributions – splayed, looped, or bundled – generally persists for several minutes. These configurations are generated by a variety of microtubule behaviors. A splayed distribution can be generated either by the growth and shrinkage of polymer in random directions (Fig. 7), by the dissociation of a bundle (Fig. 11, 210 s), or by the straightening of microtubule loops (Fig. 9, 350–455 s). In this paper we used the word splayed to refer to a distribution of spread microtubules that appears to be dominated by growth and shrinkage. Looped microtubules appear to be generated by the forward translocation of polymer into the growth cone (Fig. 6). Microtubule bundles in the growth cone can form either by the coalescence of splayed or looped microtubules (Figs. 9 and 11), or by the extension of microtubules from a preexisting bundle (Fig. 10). The origins of such distributions are difficult to infer from fixed specimens, but instead require knowledge of the history of the microtubules in the growth cone.

### *The Generation of Microtubule Polymer in the Growth Cone*

***The Role of Microtubule Dynamics.*** In theory, the properties of microtubules in extending neurites could be very different from their properties in other cells. In fibroblast cells, for example, there is rapid turnover of microtubule polymer by dynamic instability, but the overall quantity of microtubules is at or near steady state. By contrast, during axon outgrowth the cell volume increases as the growth cone moves away from the cell body, and total polymer must increase. For example, a *Xenopus* neuron can generate 150 $\mu$m of new axon per hour, requiring the assembly of perhaps 5 pg of tubulin – more tubulin than is present in a typical mammalian fibroblast cell. It is not known where this net assembly occurs or how the different requirements of the neuron affect the dynamics of microtubule polymerization and depolymerization or the transport of tubulin.

In principle, by measuring the four dynamic parameters (growth, shrinkage, catastrophe, and rescue rates) of a significant number of microtubules in the growth cone, we could assess whether net growth of microtubules occurred via growth of microtubules in the growth cone. Such an assessment has been limited by our ability to measure only a small proportion of microtubules and our inability to determine rescue frequency in these growth cones because of high microtubule density in the central region, and because of lateral movements.

The three dynamic parameters – growth rate, shrinkage rate, and catastrophe rate – that we could measure were similar to those found in other systems (Table I) where a mass balance of microtubules is maintained, and where there is no net growth over time. Though our measurements encompass a small proportion of microtubules, this suggests that if net growth of microtubules in the growth cone were occurring, it probably occurs through the modulation of rescue rates, a parameter which we were unable to measure directly.

An indirect measurement of rescue rates based on the number of growing microtubules, the number of shrinking microtubules, and the catastrophe frequency also indicates that microtubules in the growth cone may have high rescue frequencies. We can determine whether there is net growth (increase in polymer mass) of a microtubule array by examining the average behavior of the microtubules of the array although such an analysis will not tell us anything about the distribution or the fluctuations of the array. On average, microtubules in the growth cone grow for 1.39 min to a length of 14.6 $\mu$m (10.53 $\mu$m/min average growth rate, 0.72 $min^{-1}$ catastrophe frequency) before they transit to a shrinking phase and depolymerize at a rate of 9.8 $\mu$m/min. If mass balance were maintained, and these microtubules (or the average microtubule) showed no net growth, the rescue frequency would have to be 0.67 $min^{-1}$. If rescue were to occur on average in less than 14.6 $\mu$m, there would be net growth or if in more than 14.6 $\mu$m there would be net depolymerization.

In the growth cone, we have not been able to directly measure rescue frequencies. However, we can calculate the rescue frequency from the number of growing microtubules, the number of shrinking microtubules, and the catastrophe frequency. At steady state the number of microtubules growing at any time, $n_g$, and the number shrinking at any time, $n_s$, is related to the first order growing to shrinking transition, $k_c$ (for catastrophe) and $k_r$ (for rescue) by the equation: $n_g/n_s = k_r/k_c$ (Mitchison and Kirschner, 1987). We have found that the ratio of growing to shrinking microtubules in the growth cone is 2.4 (determined in 105 frames, for two neurons) resulting in a calculated $k_r$ of 1.74 $min^{-1}$.

From this rescue frequency we can say that, on average,

microtubules in the growth cone grow for 1.39 min to a length of 14.6 μm before they transit to a shrinking phase and depolymerize at a rate of 9.8 μm/min and shrink 5.6 μm before being rescued. This would produce net growth or 9 μm for a 2-min excursion of growth and shrinkage. In terms of the dimensions of an average growth cone, such a microtubule would grow from a region close to the neck of the growth cone out to the periphery, and shrink back into the densely populated central region.

The accuracy of the calculated rescue frequency and subsequent calculations depend on our ability either to measure all growing and shrinking microtubules or to estimate accurately the fraction of microtubules that are growing or shrinking and to determine that such events are actually occurring through polymerization and depolymerization, rather than through polymer translocation. These estimates are therefore very crude. Furthermore, because the calculation assumes steady-state conditions, it does not account for new nucleation of microtubules. In the growth cone, these factors are largely unknown, and for these reasons, we cannot quantitatively determine how much growth actually occurs through polymerization in the growth cone.

These calculations are not accurate enough for us to determine the contribution of polymerization to the net extension of the microtubule array, but they do provide a tool for thinking about possible mechanisms of polymer growth. Given the high rescue rates expected from the calculations and the rarity of rescue observed in the periphery, we might expect that rescue is frequent in microtubule bundles, where we could not resolve single microtubules. The progressive advance of microtubule bundling during axon formation, and the formation of microtubule bundles in the growth cone as it advances could generate a forward wave of the stabilizing (rescuing) activity. In this way, the bundling of microtubules would play a role not only in restricting the microtubules to an axonal configuration, but also in driving net polymer growth.

*Translocation of Polymer.* Our observations suggest that new polymer in the growth cone is also generated by assembly within the cell body or the axon and subsequent translocation into the growth cone. Although we could not find or make fiduciary marks directly on the growth cone microtubules, we have seen clear, indirect indications that such a process occurs. In many circumstances we observed the forward movement of coherent arrays of microtubules within the growth cone. Microtubule polymerization could not have caused simultaneous movements of microtubule loops that were in different regions of the growth cone. The forces acting on microtubules that cause them to loop and bend are also best explained by the forward translocation of microtubules against a barrier. Although increasing contour length and bending could be explained by growth against a barrier, the combination of backward movement of microtubule ends, and the forward movement of the forming loops make this possibility unlikely, in our view.

The coordinate nature of the polymer translocation that we observe resembles the translocation of polymer observed by Reinsch et al. (1991) using photoactivation in the axons of *Xenopus* neurons. We measured rates of translocation as high as 10 μm/min over short intervals of <1 min. This polymer translocation rate in the growth cone is faster than the overall rate of 1 μm/min found in the axon (Reinsch et al., 1991). However, it should be noted that the neurons used by Reinsch et al. (1991), most of which were dissociated from the neural tube, had about half the growth rates than the explanted neurons used here. In addition, they found that instantaneous rates were quite variable and often high especially near the growth cone, while those averaged over 30 min were slower. We only measured translocation when it was rapid and significantly exceeded the rate of growth cone advance and made no effort to calculate time-averaged translocation rates. For this reason, we cannot quantitatively estimate the contribution of translocation to the generation of new polymer.

### *The Coupling of Growth Cone Advance and Microtubule Extension*

During axon elongation, the growth cone moves forward and the membrane behind it collapses, becomes quiescent, and forms new axonal structure. Over time, the microtubules must elongate equal to the rate of growth cone movement. If microtubule growth and growth cone movement were tightly coupled, the density of microtubules in the growth cone would be constant. We observed, however, that the configuration of microtubules as well as the amount of microtubule polymer in the growth cone is not constant. Furthermore, the shape of the growth cone does not always reflect the microtubule array. Such observations indicate that the advance of the growth cone and the extension of the microtubule array are not strictly coordinated.

The generation of the various microtubule configurations appears, in some respects, to reflect the relationship between the rate of microtubule extension, and the rate of growth cone advance. Fig. 14 illustrates the three types of microtubule distributions that we observed and the predicted relationship between microtubule translocation, microtubule bundling, and growth cone advance. When microtubules in the growth cone are splayed (growth cone A), the amount of polymer in the growth cone appears to remain constant, and we do not see obvious signs of polymer translocation into the growth cone (see Fig. 7). Single microtubules appear to grow and shrink independently and fill the space of the growth cone. These observations suggest that during splaying, the rate of microtubule polymer translocation (*arrows* on microtubules) matches the rate of growth cone advance (*arrow* leading the growth cone), and that bundling is primarily restricted to the axon or the neck of the growth cone. It is also possible that translocation is slower than growth cone advance, and that additional polymer is generated by net growth of microtubules in the growth cone; unfortunately the detailed mass balance is impossible to extract from our data.

During looping (growth cone B), the amount of polymer in the growth cone increases and the microtubules appear to be under compression. We believe that the increase in polymer, and the formation of loops is best explained by the translocation of polymer into the growth cone without compensating depolymerization. Furthermore, after the loops have formed, they are translocated forward within the growth cone. Altogether, these observations suggest that during looping, the rate of polymer translocation exceeds the rate of growth cone advance, but that microtubule bundles are still restricted to the axon.

Microtubule bundling (growth cone C) can occur through the coalescence of splayed microtubules, by the extension of looped microtubules, or the extension of a preexisting bundle. Because the microtubules do not loop or form bends, they do not appear to be under high compressive forces. This is most clearly seen as looped microtubules unfold and extend during conversion to microtubule bundles. This suggests that the rate of microtubule polymer translocation is slower or the same as growth cone advance, and that this allows bundling to occur within the growth cone.

These models predict that the relative rates of polymer translocation and growth cone advance determine the microtubule configuration in the growth cone. Polymer translocation rates appear to be highly variable near the growth cone (Reinsch et al., 1991), and there appears to be only a loose coupling of polymer translocation and growth cone advance. The exact nature of the relationship between growth cone advance and polymer translocation remains to be determined.

### *Microtubule Bundling May Be the Critical Step in Converting the Growth Cone into New Axonal Structure*

We have seen on several occasions that the bundling of microtubules in the growth cone precedes the constriction of the membrane and consequent formation of new axon. Therefore, the formation of bundles cannot depend on physical squeezing by the cortex around the microtubules, although it is possible that microtubule bundling is caused by the constriction of an internal structure that is invisible to us. We cannot say whether microtubules actually cause the collapse of the cortex or whether both are caused by another event. The organization of microtubules may in fact feed back on the actin cortex, since microtubule depolymerizing drugs can stimulate growth cone-like activity along the axon (Bray, 1978). Bundling, therefore, may be the first morphological event related to axon formation.

### *Microtubule Placement May Be an Early Event in Growth Cone Turning*

Although in this study we have not focused on pathfinding in response to natural cues, we have examined some cases where neurons spontaneously turned. The microtubule polymer events in turning neurons were similar to those found in neurons that were growing straight. The difference was that with turning neurons, microtubule polymer was laid down in a new direction. In several examples we found that there were changes in the orientation of the microtubule array that signified the direction of turning before the growth cone showed obvious signs of asymmetry. While it is not surprising that the microtubules adopt an orientation consistent with the ultimate direction of the neuron, it is important that in several cases the microtubule reorganization preceded obvious changes in overall growth cone morphology. This does not prove that microtubules respond directly to extracellular cues for turning, since there may be a whole sequence of invisible events that precede the asymmetric microtubule organization. However, these other processes must have an early effect on microtubule polymer organization.

The sequence of events that we observed in these spontaneously turning neurons resembles those found in growth cones that were making turns in response to physiological turning cues. In an accompanying paper, Sabry et al. (1991) used similar methods of microinjection of fluorescently labeled tubulin to study the pathfinding process of pioneer neurons in the grasshopper leg. Although visualization in this system was more difficult due primarily to the unevenness of the natural epithelial substrate, the turning signals in this system were more physiological. In these neurons, an asymmetric distribution of microtubules was also generated very early in the response of these neurons to specific external turning cues, before any obvious asymmetry could be seen in the overall shape of the growth cone. It will be particularly interesting to study the processes of microtubule dynamics in the grasshopper neurons at the resolution we have employed here. Similarly, we would like to study the response of *Xenopus* neurons to external signals generated by the substrate or by chemotactic agents. Such studies could examine whether asymmetric microtubule bundling is a causal agent only during the spontaneous turning seen here, or whether these early microtubule redistributions are an obligate part of the normal turning response of neurons to external signals.

In the past it had been convenient to separate the process of axonal growth from the process of pathfinding. Axonal growth was defined as the laying down of new structures in the axon of which microtubules are the most prominent. Pathfinding was defined as an event in the growth cone that biased axonal growth in response to extracellular signals. The assumption that the microtubule cytoskeleton was restricted to the axon implied that its major role was to provide dimensional support. The assumption that the actin cytoskeleton, though not restricted to the growth cone, played its most active role there implied that actin was involved in shaping of the growth cone. For primary *Xenopus* neurons in culture this distinction is untenable. Microtubules are found both in the axon and deep in the growth cone. During axon elongation they assume a series of configurations in the growth cone indicating that the microtubule array does not merely elongate in response to growth cone movements generated by the actin cortex. Most importantly, it appears that microtubule bundling in the growth cone is the critical event in converting the typical organization of tubulin in the growth cone to the very different organization in the axon. Similarly, in turning, the early orientation and bundling of microtubules in the new direction of growth suggests that these events are important to directing axon growth. These observations, and the ability to observe microtubules with high time resolution in these living neurons has set the stage for a more precise understanding of the interaction between microtubules and other important elements that control axon elongation and pathfinding. We can now begin to determine how directly growth and turning cues act on microtubules. In addition, it will be interesting to define the interaction of microtubules with other components of the cytoskeleton, such as actin.

We would like to thank Tim Mitchison and David Drechsel for valuable advice and encouragement throughout this work. We are deeply grateful to Dr. Louis F. Reichardt for allowing us to use his microscope and Dr. John Sedat, Dr. David Agard, Jason Swedlow, Hans Chen, and Dr. Jon Minden for their generosity and patience in teaching us how to use their CCD acquisition and analysis systems. We wish to thank Douglas McVay for constructing modifications for the sealed chamber; the growth cone collective, James Sabry and Sigrid Reinsch, for helpful comments and discussion throughout; and Andrew Murray, Jeremy Minshull, Douglas Kellogg, and Michael Glotzer for critical readings of the manuscript.

These studies were supported by a grant from the National Institutes of General Medical Sciences to M. W. Kirschner.

Received for publication 17 May 1991 and in revised form 24 June 1991.

### *References*

Belmont, L. D., A. A. Hyman, K. E. Sawin, and T. J. Mitchison. 1990. Real-time visualization of cell cycle-dependent changes in microtubule dynamics in cytoplasmic extracts. *Cell.* 62:579–589.

Bentley, D., and A. Toroian-Raymond. 1986. Disoriented pathfinding by pioneer neurone growth cones deprived of filopodia by cytochalasin treatment. *Nature (Lond.).* 323:712–715.

Bray, D. 1978. Growth cone formation in cultures of sensory neurons. *Proc. Natl. Acad. Sci. USA.* 75:5226–5229.

Bridgman, P. C., and M. E. Dailey. 1989. The organization of myosin and actin in rapid frozen nerve growth cones. *J. Cell Biol.* 108:95–109.

Bunge, M. B. 1973. Fine structure of nerve fibers and growth cones of isolated sympathetic neurons in culture. *J. Cell Biol.* 56:713–735.

Cassimeris, L., N. K. Pryer, and E. D. Salmon. 1988. Real-time observations of microtubule dynamic instability in living cells. *J. Cell Biol.* 107:2223–2231.

Chen, H., J. Sedat, and D. A. Agard. 1989. Manipulation, Display, and Analysis of Three-dimensional Biological Images. *In* The Handbook of Biological Confocal Microscopy. J. Pawley, editor. IMP Press, Madison, WI. 127–135.

Cheng, T. P. O., and T. S. Reese. 1985. Polarized compartmentalization of organelles in growth cones from developing optic tectum. *J. Cell Biol.* 101:1473–1480.

Daniels, M. P. 1972. Colchicine inhibition of nerve fiber formation in vitro. *J. Cell Biol.* 53:164–176.

Forscher, P., and S. J. Smith. 1988. Actions of cytochalasins on the organization of actin filaments and microtubules in a neuronal growth cone. *J. Cell Biol.* 107:1505–1516.

Gard, D. L., and M. W. Kirschner. 1987. A microtubule-associated protein from *Xenopus* eggs that specifically promotes assembly at the plus-end. *J. Cell Biol.* 105:2203–2215.

Goldberg, D. J., and D. W. Burmeister. 1986. Stages in axon formation: observations of growth of *Aplysia* axons in culture using video-enhanced contrast-differential interference contrast microscopy. *J. Cell Biol.* 103:1921–1931.

Harris, W. A., C. E. Holt, T. A. Smith, and N. Gallenson. 1985. Growth cones of developing retinal cells in vivo, on culture surfaces, and in collagen matrices. *J. Neurosci. Res.* 13:101–122.

Harrison, R. G. 1910. The outgrowth of the nerve fiber as a mode of protoplasmic movement. *J. Exp. Zool.* 17:521–544.

Heidemann, S. R., J. M. Landers, and M. A. Hamborg. 1981. Polarity orientation of axonal microtubules. *J. Cell Biol.* 91:661–665.

Hinkle, L., C. D. McCaig, and K. R. Robinson. 1981. The direction of growth of differentiating neurones and myoblasts from frog embryos in an applied electric field. *J. Physiol.* 314:121–135.

Hyman, A. A., D. N. Drechsel, D. Kellogg, S. Salser, K. Sawin, P. Steffan, L. Wordeman, and T. J. Mitchison. 1991. Preparation of modified tubulins. *Methods Enzymol.* 196:478–485.

Lankford, K. L., and W. L. Klein. 1990. Ultrastructure of individual neurons isolated from avian retina: occurrence of microtubule loops in dendrites. *Brain Res. Dev. Brain Res.* 51(2):217–224.

Marsh, L., and P. C. Letourneau. 1984. Growth of neurites without filopodial or lamellipodial activity in the presence of cytochalasin B. *J. Cell Biol.* 99:2041–2047.

Mitchison, T., and M. Kirschner. 1988. Cytoskeletal dynamics and nerve growth. *Neuron.* 1:761–772.

Mitchison, T. J., and M. W. Kirschner. 1987. Some thoughts on the partitioning of tubulin between monomer and polymer under conditions of dynamic instability. *Cell Biophys.* 11:35–55.

Newport, J., and M. W. Kirschner. 1982. A major developmental transition in early *Xenopus* embryos. I. Characterization and timing of cellular changes at the midblastula stage. *Cell.* 30:675–686.

Nieuwkoop, P. D., and J. Faber. 1956. Normal table of Xenopus laevis. Amsterdam: North-Holland.: *Daudin.* 168–170.

Peters, A., S. L. Palay, and H. Webster. 1991. The fine structure of the nervous system: neurons and their supporting cells. Oxford University Press, New York. 101–137.

Porter, K. R. 1966. Cytoplasmic microtubules and their functions. *In* Principles of Biomolecular Organization. G. E. W. Wolstenholme and M. O'Connor, editors. Little, Brown, and Co., Boston. 308–356.

Ramon y Cajal, S. 1890. Sur l'origine et les ramifications des fibres nerveuses de la moelle embryonaire. *Anat. Anz.* 5:609–613.

Reinsch, S. S., T. J. Mitchison, and M. W. Kirschner. 1991. Microtubule polymer assembly and transport during axonal elongation. *J. Cell Biol.* 115: 365–379.

Sabry, J. H., T. P. O'Connor, L. Evans, A. Toroian-Raymond, M. W. Kirschner, and D. Bentley. 1991. Microtubule behavior during guidance of pioneer neuron growth cones in situ. *J. Cell Biol.* 115:381–395.

Sammak, P. J., and G. G. Borisy. 1988. Direct observation of microtubule dynamics in living cells. *Nature (Lond.).* 332:724–726.

Schnapp, B. J., and T. S. Reese. 1982. Cytoplasmic structure in rapid-frozen axons. *J. Cell Biol.* 94:667–679.

Schulze, E., and M. Kirschner. 1988. New features of microtubule behaviour observed in vivo. *Nature (Lond.).* 334:356–359.

Tsui, H. T., K. L. Lankford, H. Ris, and W. L. Klein. 1984. Novel organization of microtubules in cultured central nervous system neurons: formation of hairpin loops at ends of maturing neurites. *J. Neurosci.* 4:3002–3013.

Walker, R. A., E. T. O'Brien, N. K. Pryer, M. F. Soboeiro, W. A. Voter, H. P. Erickson, and E. D. Salmon. 1988. Dynamic instability of individual microtubules analyzed by video light microscopy: rate constants and transition frequencies. *J. Cell Biol.* 107:1437–1448.

Yamada, K. M., B. S. Spooner, and N. K. Wessells. 1971. Ultrastructure and function of growth cones and axons of cultured nerve cells. *J. Cell Biol.* 49:614–635.